# Continuous Probabilistic Nearest-Neighbor Queries for Uncertain Trajectories

Goce Trajcevski
Department of EECS
Northwestern University
goce@eecs.northwestern.edu

Roberto Tamassia[*]
Department of CS
Brown University
rt@cs.brown.edu

Hui Ding
Department of EECS
Northwestern University
hdi117@eecs.northwestern.edu

Peter Scheuermann[†]
Department of EECS
Northwestern University
peters@eecs.northwestern.edu

Isabel F. Cruz[‡]
Department of CS
University of Illinois at Chicago
ifc@cs.uic.edu

## ABSTRACT

This work addresses the problem of processing continuous Nearest Neighbor (NN) queries for moving objects trajectories when the exact position of a given object at a particular time instant is not known, but is bounded by an uncertainty region. As has already been observed in the literature, the answers to continuous NN-queries in spatio-temporal settings are time parameterized in the sense that the objects constituting the answer vary over time. Incorporating uncertainty in the model yields additional attributes that affect the semantics of the answer to this type of queries. In this work, we formalize the impact of uncertainty on the answers to the continuous probabilistic NN-queries, provide a compact structure for their representation and efficient algorithms for constructing that structure. We also identify syntactic constructs for several qualitative variants of continuous probabilistic NN-queries for uncertain trajectories and present efficient algorithms for their processing.

## 1. INTRODUCTION

Moving Objects Databases (MODs) [8] constitute a fundamental technology for a wide variety of applications that may require some type of Location Based Services (LBS) [26] for mobile entities. The main tasks associated with MODs are: (1) the efficient management of the location-in-time information associated with mobile entities; (2) the efficient processing of various queries of interest, such as range or nearest neighbor (NN) queries. However, as has already been observed in the literature [4, 22], due to the imprecision of positioning technologies (e.g., roadside sensors, GPS), it is not always possible to ascertain the exact location of a particular moving object. Hence, *uncertainty* must be taken into account in the *data models*, in the *linguistic constructs* of the queries, and in the *processing algorithms*. The impact of various sources of imprecision in the context of probabilistic and uncertain data management has received considerable attention recently (e.g., [31, 21]), including spatial and spatio-temporal settings (e.g., [4, 22, 35, 36]).

Contrary to what happens in pure spatial settings [10, 24], the answer to a *continuous* NN-query in a spatio-temporal setting is *time parameterized* [34, 33] in the sense that the actual nearest neighbor of a given object need not be the same throughout the time interval of interest. As an example, assume that we have a MOD which consists of a set of trajectories: $\mathcal{S} = \{Tr_1, Tr_2, \ldots, Tr_N\}$, and a query $\mathbf{Q\_nn(q)}$: *"Retrieve the nearest neighbor of the moving object whose trajectory is $Tr_q$ between $t_b$ and $t_e$".* The answer to the query is represented as a sequence $\mathbf{A\_nn(q)}$: $[(Tr_{i1}, [t_b, t_1]), (Tr_{i2}, [t_1, t_2]), \ldots, (Tr_{im}, [t_{m-1}, t_e])]$, expressing the fact that $Tr_{i1} \in \mathcal{S}$ is the nearest neighbor of $Tr_q$ initially and up to time $t_1$. However, the nearest neighbor of $Tr_q$ during the time interval $[t_{k-1}, t_k] \subseteq [t_b, t_e]$ $(k > 1)$ is the trajectory $T_{ik} \in \mathcal{S}$.

At the heart of the motivation for this work is the observation that incorporating *uncertainty* in the representation of the trajectories must be properly reflected in the syntax of both NN-queries and of their respective answers. For example, consider a simple extension to $\mathbf{Q\_nn(q)}$, in a manner that includes some uncertainty awareness, $\mathbf{UQ\_nn(q)}$: *"Retrieve all the objects that have a non-zero probability of being a nearest neighbor to the moving object $Tr_q$, between $t_b$ and $t_e$".* In this case, in addition to a trajectory, e.g., $Tr_{i1}$ being the nearest neighbor of $Tr_q$ during $[t_b, t_1]$, it may well be that some other objects may have a non-zero probability of being a nearest neighbor of $Tr_q$ in some sub-intervals of $[t_b, t_1]$.

**Example 1.** *Consider the scenario depicted in Figure 1. It*

[*] Research supported in part by NSF Awards IIS–0324846, IIS–0713403 and OCI–0724806.

[†] Research supported in part by NSF Award IIS-0325144/003.

[‡] Research supported in part by NSF Awards ITR IIS-0326284, IIS-0513553, and IIS-0812258.

*illustrates 4 trajectories: $Tr_1$, $Tr_2$, $Tr_3$, and $Tr_q$, shown as 3D line segments; and possible bounds of the uncertainties of their locations, shown as sheared cylinders. Ignoring the uncertainty, the nearest neighbor of $Tr_q$ is $Tr_1$ in $[t_b, t_1]$, and $Tr_2$ in $[t_1, t_e]$. However, if location uncertainty is taken into consideration, we see that not only $Tr_1$, but also $Tr_3$ has a non-zero probability of being the nearest neighbor to $Tr_q$ at $t = t_{b1}$. Similarly, at $t = t_{11}$ all three trajectories have non-zero probabilities.*

Clearly, this needs to be considered continuously throughout the entire duration of $[t_b, t_e]$. However, it is even more important that we properly reflect it into all the sub-intervals, at a level of granularity dictated by the particular problem setting.

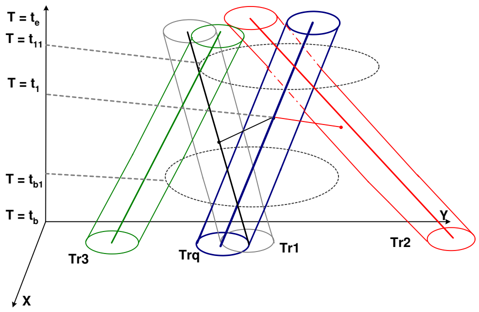

**Figure 1: Continuous nearest neighbor for uncertain trajectories.**

We postulate that the structure of the answer, **UA_nn(q)**, needs to be organized in a way that:

- It identifies the trajectories $Tr_{i1}$, $Tr_{i2}$, $\ldots$, which have the *highest probability* of being the nearest neighbor to $Tr_q$, and the corresponding time intervals $[t_b, t_1]$, $[t_1, t_2]$, $\ldots$.
- It identifies *sub-intervals* within each $[t_{k-1}, t_k]$ during which a particular trajectory would have been ranked as the one with highest probability nearest neighbor of $Tr_q$, had it not been for $Tr_{ik}$.
- The structure is recursively refined for each sub-interval of time, until no lower granularity exists containing trajectories with non-zero probability of being a nearest neighbor to $Tr_q$.

Each component of the answer may be augmented by an extra *descriptor* of the properties of the probability values of the trajectory associated with the particular time interval. For instance, such descriptors may contain: coefficients/functions of an analytical expression (if possible), *min*/*max* values, plus a discrete sequence of values of the probability at time instants within the given interval, etc.

To represent the structure of **UA_nn(q)**, we propose an *interval tree* in which:

- The root consists of the parameters of the query (i.e., query trajectory $Tr_q$ and the time interval $[t_b, t_e]$).
- The children of each internal node are the nodes that, with the exclusion of their parents, have the highest probability of being the nearest neighbors of $Tr_q$, within the time interval bounded by the parent.

The structure of each internal or leaf node consists of the following attributes:

1. time-interval $[t_i, t_{i+1}]$ of relevance;
2. unique *ID*, say, $Tr_i$, of the trajectory corresponding to the answer during the time-interval $[t_i, t_{i+1}]$;
3. *descriptor* $D_i$ of the properties of the probability of $Tr_i$ being the nearest neighbor to $Tr_q$ within $[t_i, t_{i+1}]$; and
4. pointers to the children-trajectories that have the next-highest probability of being the nearest neighbor within the disjoint sub-intervals of $[t_i, t_{i+1}]$.

Clearly, this type of tree need not be balanced in terms of the height and number of children for each internal node, but we note that the leaf nodes correspond to the trajectories that have the smallest probability of being an uncertain nearest neighbor of $Tr_q$ within the corresponding time-intervals (i.e., no other trajectory has a smaller non-zero probability). We call this tree *IPAC-NN* (Interval-based Probabilistic Answer to a Continuous NN query) and we illustrate it in Figure 2. We note that if the root of the tree is removed, in effect we have a Direct Acyclic Graph (DAG), which represents the answer. Given this declarative description of the semantics of the answer to a continuous probabilistic NN-query, the focus of the rest of this work is on the procedural counterpart: constructing the *IPAC-NN* tree for a given query. We note that we do not address the issue of calculating the descriptors $D_i$ of the individual nodes. Instead, we concentrate on *ranking* [30]. In addition to formalizing the semantics of the structure of the answers to continuous probabilistic NN-queries for uncertain trajectories, our main contributions can be summarized as follows:

- We identify a simple transformation of a view over the uncertain trajectories, which enables a construction of the *relative ranking* of the probabilistic values for instantaneous uncertain NN-queries.
- We demonstrate that our transformation is applicable to a large class of probability density functions (*pdf*s) that describe the uncertainty associated with the location.
- We develop efficient algorithms to construct a geometric dual of a IPAC-NN tree.
- We identify several syntactic variants for systematic incorporation of uncertainty in the statement of the continuous NN-queries; for each variant we present an efficient algorithm for its processing, based on the dual of the IPAC-NN tree.
- We present experimental observations demonstrating the benefits of our approach.

The rest of this paper is structured as follows. In Section 2, we gather the necessary background. Section 3 presents the main contribution of our work in terms of the transformation of the uncertain trajectories and its implication towards algorithmic construction of the IPAC-NN tree, as well as identifying the class of (instantaneous) location *pdf*s for which the transformation is applicable. In Section 4, we present the different variants of the continuous probabilistic NN-queries and their processing. Section 5 presents our experimental observations and Section 6 positions our work with respect to the related literature. Finally, in Section 7, we give some concluding remarks and outline directions for future work. For clarity of the presentation, we have moved the lengthier proofs to an Appendix.

## 2. PRELIMINARIES

In this section, we introduce the background necessary for the development of our main results. First, we define the model of uncertain trajectories used throughout this work. Subsequently, we recollect some results pertaining to instantaneous NN-queries for uncertain objects for the special case when the querying object is *crisp* (i.e., its location is exact, without any uncertainty) [4].

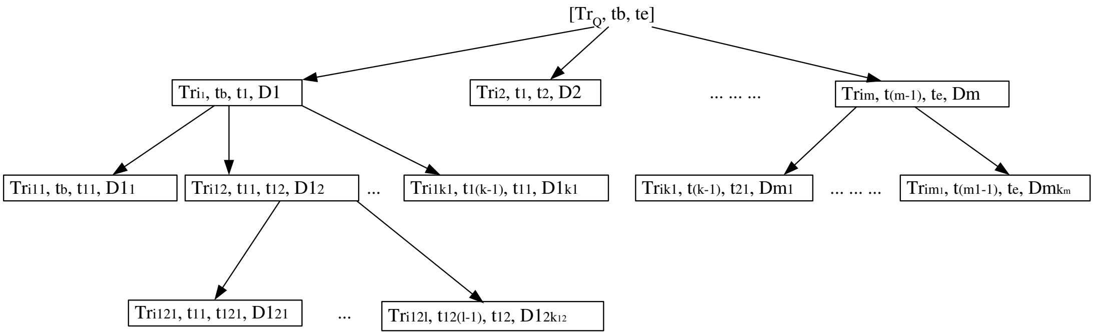

**Figure 2: Interval tree of the answer to a probabilistic continuous NN-query.**

## 2.1 Uncertainty of Motion

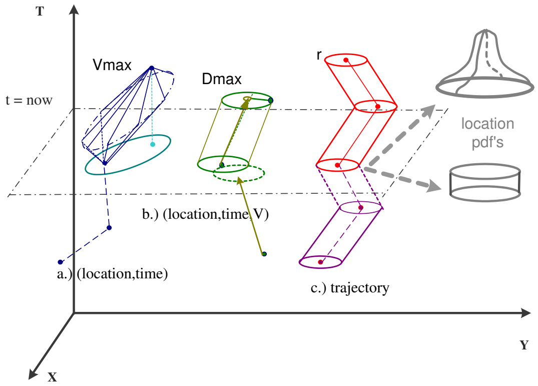

**Figure 3: Motion models and uncertainty.**

Selecting the model for the motion plan of the moving objects affects not only the algorithms for processing the popular categories of spatio-temporal queries (e.g., range, NN) [8], but also the representation of uncertainty. For example, assume that the moving objects sends periodic updates of the form $(x, y, t)$ reporting its $(x, y)$ location (obtained, for example, using an on-board GPS system) at time $t$ to the MOD server [18]. Given an upper-bound on its maximum speed $v_{max}$, the location in between two updates is bounded by an ellipse (Figure 3.a) [11, 22]. On the other hand, if along with its current (sampled) location the object also transmits its *expected* velocity then, for as long as its sampled location of the object at a given time does not deviate more than a certain threshold, say $D_{max}$, from its expected location, it needs not transmit an update to the server. This is called a *dead-reckoning* policy [37], and the possible whereabouts are illustrated in Figure 3.b.

Our work assumes that each moving object has a *full trajectory* as its motion model. This corresponds to the settings in which users transmit to the MOD server: (1) the *beginning location*; (2) the *ending location*; (3) the *beginning time*; and (4) possibly a set of points to be visited. Based on the information available at the electronic maps, along with the traffic patterns, the server constructs the *shortest travel time* or *shortest path* trajectory, and transmits it back the user, keeping a copy in the server for query processing [9]. Aside from the large number of commercial fleet vehicles (e.g., FedEx, UPS) the number of shortest travel time trajectories requested by individual users, from services such as MapQuest, Yahoo Maps and Google Maps, exceeded 85,000,000 per month in 2006 [6]. The uncertainty model with the full trajectory is often based on the assumption that at each time instant there is a bound on the object's possible whereabouts [36], as shown in Figure 3.c. This figure also illustrates that at a given time instance, the *pdf* of the location of the object within its boundaries may take different forms (e.g., uniform, bounded-Gaussian).

Formally, a *trajectory* is a function $Time \rightarrow \mathcal{R}^2$, represented as a sequence of 3D (2D spatial plus Time) points, accompanied by a unique ID of the moving object: $Tr_i = \{oid_i, (x_{i_1}, y_{i_1}, t_{i_1}), (x_{i_2}, y_{i_2}, t_{i_2}), \ldots, (x_{i_k}, y_{i_k}, t_{i_k})\}$ where $t_{i_1} \leq t_{i_2} \leq \ldots \leq t_{i_k}$. When clear from the context, we will interchangeably use $Tr_i$ and $oid_i$. In between two consecutive points, the location of the object $oid_i$ at time $t \in (t_{i_{(k-1)}}, t_{ik})$ is obtained by linear interpolation, assuming that the object is moving along a straight line-segment and with a constant speed that is calculated as:

$$v_{i_k} = \frac{\sqrt{(x_{i_k} - x_{i_{(k-1)}})^2 + (y_{i_k} - y_{i_{(k-1)}})^2}}{t_{i_k} - t_{i_{(k-1)}}} \qquad (1)$$

An *uncertain trajectory* $Tr_i^u$ is a trajectory augmented with: (1) the information about the *radius* of the circle bounding the *uncertainty zone*, i.e., the disk representing the 2D set of possible locations of the object at a given time instant; and (2) the *pdf* of the location within the uncertainty disk. Therefore, we have: $Tr_i^u = \{oid_i, r, pdf, (x_{i_1}, y_{i_1}, t_{i_1}), (x_{i_2}, y_{i_2}, t_{i_2}), \ldots, (x_{i_k}, y_{i_k}, t_{i_k})\}$. The location of the object in the center of the uncertainty disk is now called its *expected location* and we use $D_i(t)$ to denote the uncertainty disk of $Tr_i$ at time $t$. Throughout this work, we assume the parameters $r$ and *pdf* are the same for the trajectories in a given set. As commonly assumed in the literature (e.g., [4, 35]) we also assume that, viewed as random variables, the *pdf*s of the locations of the uncertain objects are *independent* from each other. We note that in the examples we use *uniformly distributed* 2D random variables in the uncertainty zone. Assuming that the expected location of the object with $oid_k$ at time $t$ is $(x_k(t), y_k(t))$, at that time $pdf_k(t)(X, Y) =$

$$= \begin{cases} 0, & \sqrt{(x_k(t) - X)^2 + (y_k(t) - Y)^2} > r \\ \frac{1}{r^2 \pi}, & \sqrt{(x_k(t) - X)^2 + (y_k(t) - Y)^2} \leq r \end{cases} \qquad (2)$$

However, as we will formally demonstrate in Section 3, our results are applicable to a much larger class of *pdf*s.

## 2.2 Instantaneous NN-queries for Uncertain Objects and Crisp Querying Object

Assume that the location of the querying object $Tr_q$ is *crisp*, and the possible locations of the other trajectories are disks with radii $r$. A thorough treatment of this problem setting is presented in [4]. Here, we only present a concise summary, and observations that are immediately relevant to our work.

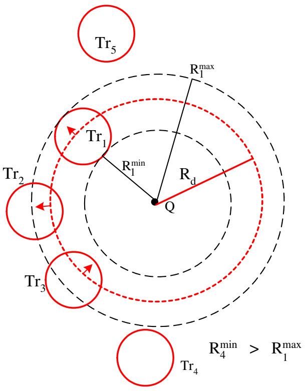

**Figure 4: Uncertain NN-query (crisp $Tr_q$).**

**I:** The distance from $Q$ to the most distant point of the closest disk, $R_{max}$, is the upper bound on the distance that any possible nearest neighbor of $Tr_q$ can have. Consequently, any $Tr_i$ whose closest possible distance to $Q$, denoted by $R_i^{min}$, is larger than $R_{max}$, has a 0 probability of being a nearest neighbor to $Tr_q$ and can therefore be safely pruned (i.e., ignored from any computation). As illustrated in Figure 4, $R_4^{min} > R_1^{max}$, and similarly $R_5^{min} > R_1^{max}$, which means that $Tr_4$ and $Tr_5$ cannot have a non-zero probability of being a nearest neighbor to $Tr_q$. We use $R_{min}$ to denote the distance from $Q$ to the closest point of the closest disk.

**II:** In general, the probability that (the location along the trajectory at a given time of) a given object $Tr_i$ is *within distance* $R_d$ from $Q(= Tr_q)$ can be specified as:

$$P_{i,Q}^{WD}(R_d) = \int_A \int pdf_i(x,y)\, dx\, dy \tag{3}$$

where $A$ is the area of the intersection of the disk with radius $R_d$ centered at $Q$ and the uncertainty disk of $Tr_i$ and $pdf_i(x,y)$ is the corresponding *pdf* of $Tr_i$.

**Example 2:** [4] *When $pdf_i(x,y)$ is uniform, the probability $P_{i,Q}^{WD}(R_d)$ can be calculated as*:

$$P_{i,Q}^{WD}(R_d) \begin{cases} 0 & \text{if}(R_d < r_{min_i}) \\ \frac{1}{R_d^2\pi}(\Theta - \frac{1}{2}\sin 2\Theta) + \frac{1}{\pi}(\alpha - \frac{1}{2}\sin 2\alpha) & \\ & \text{if}(d_{iQ} - r \le R_d \le d_{iQ} + r) \\ 1 & \text{if}(d_{iQ} + r < R_d) \end{cases} \tag{4}$$

*where* $\Theta = \arccos \frac{d_{iQ}^2 + r^2 - R_d^2}{2 d_{iQ} r}$ *and* $\alpha = \arccos \frac{d_{iQ}^2 + R_d^2 - r^2}{2 d_{iQ} R_d}$, *and $d_{iQ}$ is the distance between $Q$ and the expected location*[1] *of $Tr_i$. Taking the derivative of $P_{i,Q}^{WD}$, yields $pdf_{i,Q}^{WD}(R_d)$ which, in the case of uniform distribution, will be non-zero only when $d_{iQ} - r \le R_d \le d_{iQ} + r$.*

**III:** The probability of a given object, say $Tr_j$, being a nearest neighbor of the crisp querying object $Tr_q$ can be calculated based on the following:
(a) The probability of $Tr_j$ being within distance $\le R_d$;
(b) The probability that every other object $Tr_i (i \neq j)$ is within distance $> R_d$ from $Q$; and
(c) The fact that the distributions of the objects are assumed to be independent from each other.
The generic formula can be specified as:

$$P_{j,Q}^{NN} = \int_0^\infty pdf_{j,Q}^{WD}(R_d) \cdot \prod_{i \neq j} (1 - P_{i,Q}^{WD}(R_d))\, dR_d \tag{5}$$

We note that the boundaries of the integration need not be 0 and $\infty$ because the effective boundary of the region for which an object can be a nearest neighbor of $Q$ is the ring centered at $Q$ with radii $R_{min}$ and $R_{max}$. In addition, $pdf_{j,Q}^{WD}(R_d)$ is 0 for any $R_d < R_j^{min}$, and $1 - P_{i,Q}^{WD}(R_d)$ is 1 for $R_d < R_i^{min}$. By sorting the objects that have a non-zero probability of being nearest neighbors according to the minimal distances of their boundaries from $Q$, one can break the evaluation of (5) into several intervals (one for each $R_{min_i}$), and the computation of the $P_{j,Q}^{NN}$ can be performed in an efficient manner, based on the sorted distances and the corresponding intervals [4]. Such efficiency is especially important because the actual evaluation of the integrals like those in Equation (5), may often rely on numerical computations. In a uniform distribution this is equivalent to sorting the objects according to the distances of their respective expected locations from $Q$.

**IV:** We note that the ideas above, although intuitive, have a slight problem in the context of *soundness* vs. *completeness*. Namely, the evaluations of $P_i^{NN}(Q)$ as defined by Equation (5), do not constitute a *probability space* [7] or, in terms of classical probability, $\Sigma_{\forall i} P_{i,Q}^{NN}$ will yield a value $< 1$. The reason is that, strictly speaking, the probability of a given object being the nearest neighbor to $Tr_q$ consists of two parts:

$$P_{i,Q}^{NN} = P_{i,Q}^{NN\text{-}E} + P_{i,Q}^{NN\text{-}J} \tag{6}$$

The first part, $P_{i,Q}^{NN\text{-}E}$, denotes the *exclusive* probability that $Tr_i$ is the nearest neighbor of $Tr_q$ and is calculated in the spirit of (5). The second part, $P_{i,Q}^{NN\text{-}J}$ represents the *joint* probability and corresponds to the case(s) in which $Tr_i$ is the nearest neighbor of $Tr_q$ along with some other $Tr_j$'s. Strictly speaking, it consists of the following sums:

- $\Sigma_j \int_0^\infty pdf_{i,Q}^{WD}(R_d) \cdot pdf_{j,Q}^{WD}(R_d) \cdot \prod_{k \neq i,j} (1 - P_{k,Q}^{WD}(R_d))\, dR_d$– corresponding to the cases when $Tr_i$ is a *paired*-NN with other $Tr_j$'s;
- $\Sigma_k \int_0^\infty pdf_{i,Q}^{WD}(R_d) \cdot pdf_{j,Q}^{WD}(R_d) \cdot pdf_{k,Q}^{WD}(R_d) \cdot \prod_{l \neq i,j,k} (1 - P_{l,Q}^{WD}(R_d))\, dR_d$ – capturing all the cases of triplets of trajectories being the nearest neighbor to $Tr_q$;
- ...
- $\int_0^\infty \prod_i pdf_{k,Q}^{WD}(R_d)\, dR_d$–calculating the probability that all trajectories can simultaneously be nearest neighbors.

## 3. MOVING CONVOLUTIONS AND CONTINUOUS NN-QUERIES

In this section, we present a first set of results of our work. First, we illustrate the problems that arise when the query object has an uncertainty associated with its location. Next, by using a simple transformation, we show that for a large class of *pdf*s, we can reduce this case to one in which the ideas presented in Section 2.1 can be applied almost unmodified. We subsequently present a methodology for constructing the geometric dual of the IPAC-NN tree.

[1] Appropriate modifications are needed when $Q$ is located inside the uncertainty zone of $Tr_i$ [4].

### 3.1 Within Distance: Uncertain Querying Object

For the time being, let us still consider a "snapshot" query in which the location of the querying object $Tr_q$ is also uncertain, and can be anywhere within the disk of radius $r$ centered at the expected location $Q$.

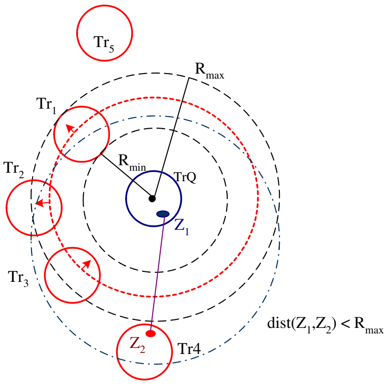

**Figure 5: Uncertain NN-query (uncertain $Tr_q$).**

The first observation is that we can no longer prune the objects whose uncertainty disk is further than $R_{max}$ from $Q$. An illustration is provided in Figure 5. Namely, when $Tr_q$ is located somewhere in the zone denoted by $Z_1$ inside of its own uncertainty disk and $Tr_4$ is located somewhere in the zone denoted by $Z_2$, their distance is $< R_{max}$ and, consequently, $Tr_4$ has a non-zero probability of being a (possible) nearest neighbor of $Tr_q$. This fact complicates the main benefits in terms of compactness of the representation and the efficiency of processing probabilistic NN-queries with respect to using the formulas from Section 2.2 (cf. [4]). Strictly speaking, at the heart of the problem is the calculation of the probability that a given object $Tr_i$ *within distance* $R_d$ of $Tr_q$.

Since the distributions of the objects within their spatial boundaries are independent, one can obtain the probability of two objects being within distance $\leq R_d$ from each other as follows:

**1.** Find the set of all the possible locations in the uncertainty disk $D_i$ that are at distance $R_d$ from *some* point in the disk $D_q$. This set is actually the intersection: $D_i \cap$ $(D_q \oplus R_d)$, where $(D_q \oplus R_d)$ denotes the *Minkowski sum* (see, e.g., [5]) of the uncertainty disk of $Tr_q$ with a disk of diameter $R_d$.

**2.** For each point $P(= (x_p, y_p)) \in D_i \cap$ $(D_q \oplus R_d)$ and a point $Q \in D_q$, evaluate $P^{WD}_{q,P}(R_d)$ using, e.g., Equation (3), and "add" the uncountably-many such results – which is, integrate over the area $D_i \cap$ $(D_q \oplus R_d)$, with $dx_p$ and $dy_p$ as the extra-variables of differentiation.

This yields a quadruple integration in the corresponding version of Equation (3) used for evaluating $P^{WD}_{i,q}(R_d)$ and yields additional overhead in determining the $pdf^{WD}_{i,q}(R_d)$ (via differentiation), in order to be able to use Equation (5) for evaluating $P^{NN}_{i,q}$. Most often, the procedure outlined above will rely on a numerical evaluation, which approximates the outer-integrals by a sum of the products of the probabilities that $Tr_i$ is at location $l_1 \in D_i$, given that $Tr_q$ is at location $l_2$, and $\|l_1 l_2\| \leq R_d$ (over all such locations $l_1$ and $l_2$, and after discretizing the corresponding location-pdf's [35, 4]). Since the locations of the individual objects are assumed to be independent, the conditional probability $Pr(Tr_i = l_1 \mid Tr_q = l_2)$ is simply $Pr(Tr_i = l_1)$.

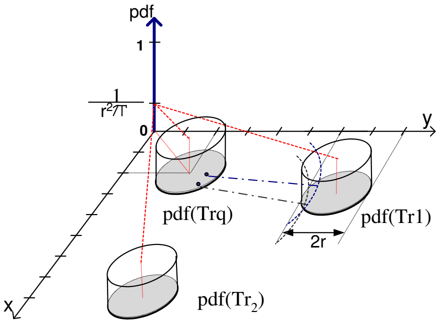

**Figure 6: Evaluating within distance probability.**

**Example 3.** *Figure 6 shows the locations of 3 uncertain objects with uniform pdf's. Each of them has the uncertainty radius of 1, and their respective expected locations are $E_{loc}(Tr_q) = (2, 2)$, $E_{loc}(Tr_1) = (7, 3)$ and $E_{loc}(Tr_2) = (3, 8)$. The two dashed segments of circles, centered at two locations inside the uncertainty disk of $Tr_q$ illustrate part of the calculation of the probability of $Tr_1$ being within distance $\leq 4$ from $Tr_q$ (obviously, 0 for $Tr_2$).*

We are now in the position to explain the theoretical foundation of our main results. Let $\overline{V}_i$ denote the 2D random variable representing the possible locations of the uncertain trajectory $Tr^u_i$ at a given time instant. Recall that the crux for evaluating a probabilistic NN-query is determining the expression for the probability of $Tr^u_i$ being within a given distance $R_d$ from $Tr^u_q$, which is, the value of $P^{WD}_i(R_d)$. An equivalent interpretation is that we need to evaluate $P(\|\overline{V}_i - \overline{V}_q\| \leq R_d)$. Now, the key observation is that $\overline{V}_i - \overline{V}_q$ is another random variable, denote it $\overline{V}_{iq}$ which, in probability and signal/image processing is known as a *cross-correlation* of $\overline{V}_i$ and $\overline{V}_q$ [17, 20]. Another interpretation is that $\overline{V}_{iq}$ can be viewed as a sum $\overline{V}_i + (-\overline{V}_q)$. Since $\overline{V}_i$ and $\overline{V}_q$ (consequently, $-\overline{V}_q$) are independent variables [4, 35]), it is a well-known fact from the probability theory that the random variable $\overline{V}_{iq}$ has a $pdf_{iq}$ which is a *convolution* of the corresponding $pdf$s of $\overline{V}_i$ and $-\overline{V}_q$) [20]. In other words:

$$pdf(\overline{V}_{iq}) = pdf(\overline{V}_i) \circ pdf(-\overline{V}_q) \quad (6)$$

**Example 4.** *As one can readily verify (cf. [20]), the convolution of two cylinders with heights $\frac{1}{r^2\pi}$ is a cone whose base is a circle with radius $2r$ and height $\frac{3}{4r^2\pi}$. As illustrated in Figure 7, instead of performing an uncountably-many additions (e.g. adding an extra outer-integration) in the context of Example 2, for the various circles of radius 4 centered somewhere in the uncertainty disk of $Tr_q$ (cf. Figure 6), we can now use a simpler calculation – evaluate the volume of the intersection of the cone centered at $(5, 1)$ $(= (7, 3) - (2, 2))$, with the cylinder with radius 4 centered at the origin (0,0).*

*Specifically, for uncertain trajectories with uniform location-pdf's, given the Equation (2), we have*

$$pdf(\overline{V}_{iq}(t)(X, Y)) = \quad (7)$$

$$\begin{cases} 0, & \sqrt{((x_i(t) - x_q(t)) - X)^2 + ((y_i(t) - y_q(t))Y)^2} > 2r \\ \frac{3}{4r^2\pi}\left(1 - \frac{\sqrt{((x_i(t)-x_q(t))-X)^2+((y_i(t)--y_q(t))Y)^2}}{2r}\right), & \text{otherwise} \end{cases}$$

We note that, in order for a convolution of two functions to exist (i.e., two functions to be *convolutable*) it is sufficient

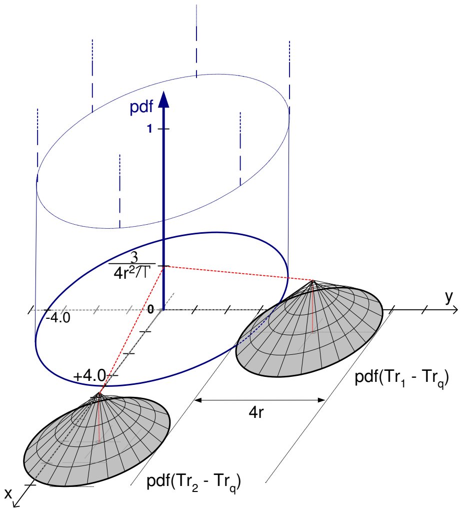

**Figure 7: Within distance probability: convolution.**

that each of them is *Lebesgue-integrable* [25]. However, in many practical settings, the *pdf*'s of the objects' locations (e.g., uniform, Gaussian) are *Riemann-integrable* [25], which is a weaker condition. Before presenting the main result, we prove some properties which demonstrate that our proposed methodology is applicable to a wide range of *pdf*s for objects' locations. For brevity, we will use $f$ to denote *pdf*$(\overline{V}_{iq})$, $g$ to denote *pdf*$(\overline{V}_i)$, and $h$ to denote the *pdf*$(-\overline{V}_q)$.

**Property 1.** *Assume that $g$ (resp. $h$) has a centroid $\overline{C}_1$ (resp. $\overline{C}_2$), which coincides with its expected value $E(\overline{V}_i)$, resp. $E(-\overline{V}_q)$. Then their convolution $f = g \circ h$ has a centroid $\overline{C}_c = \overline{C}_1 + \overline{C}_2$, and $\overline{C}_c$ is the expected value of the variable $\overline{V}_{iq}$.*

As specific examples, the expected value of the convolution of two Gaussian distributions with means $\overline{\mu}_1$ and $\overline{\mu}_2$, is exactly $\overline{\mu}_{12} = \overline{\mu}_1 + \overline{\mu}_2$, and we note that the *pdf* of the convolution is also Gaussian [20]. Similarly for the expected value of two uniform distribution, however, as we saw in Example 3, the resulting *pdf* is no longer uniform.

Property 1 provides a basis for defining the categories of *pdf*s for which our main results are applicable, and towards that end, we need to define the concept of a *rotational* (a.k.a *cylindrical*) symmetry [17]. A given 2D function, say $h$, is said to be rotationally symmetric with respect to a point $\overline{C}$ in its domain and the vertical (Z) axis if, for all other points $P$ and $Q$ in its domain, $\|\overline{PC}\| = \|\overline{QC}\| \Rightarrow h(\overline{P}) = h(\overline{(Q)})$. Now we have:

**Property 2:** *Assume that $g$ and $h$ have a rotational symmetry around their respective centers, $\overline{C}_1$ and $\overline{C}_2$, with respect to the vertical ($Z = pdf$) axis. Then, their convolution $f = g \circ h$ also has a rotational symmetry around the vertical axis and with respect to its centroid $\overline{C}_c$.*

Assume that $Tr_1^u$ and $Tr_2^u$ denote two uncertain trajectories with centers (expected locations) $C_1$ and $C_2$ at some time-instant $t$. In addition, assume that they have same (modulo translation) corresponding location *pdf*s at $t$, which are rotationally symmetric. The last claim that is needed before we state our main result for this section, is summarized in the following:

**Lemma 1:** *Let $Q$ denote a 2D point. If $\|\overline{QC}_1\| < \|\overline{QC}_2\|$, then $P_1^{NN}(Q) > P_2^{NN}(Q)$.*

Assume that we are given a collection of moving objects with equal *pdf*s (modulo translation with respect to their centers), which are rotationally symmetric. Let $Tr_q$ denote the (uncertain) querying trajectory. The main result of this section can be summarized as:

**Theorem 1.** *The permutation of the oids representing the ranking of the probabilities of individual objects being nearest neighbor to $Tr_q^u$ at a given time-instance, is exactly the same as the permutation representing the ranking of the distances of their centers (expected locations) from the center (expected location) of $Tr_q^u$.*

**Proof:** Theorem 1 is a straightforward consequence of the properties of the convolution for independent random variables with rotational symmetry, and Lemma 1.

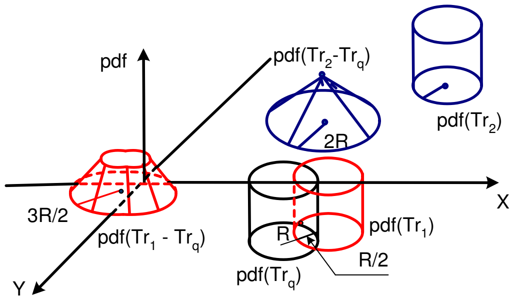

**Figure 8: Convolution of intersecting *pdf*s.**

As an illustration, recall Figure 7: – since the centroid of $Tr_1^u - Tr_q^u$ is closer to the coordinate-center than the centroid of $Tr_2^u - Tr_q^u$, we have that $P_1^{NN}(Q) > P_2^{NN}(Q)$.

We conclude this section with an observation. In the examples so far, we assumed that the uncertainty disks of the respective trajectories did not intersect. However, in practice, this need not be the case. For instance, Figure 8 shows the impact on the (*pdf* of the) resulting convolution, when a given trajectory intersects the querying trajectory. However, it can be readily demonstrated that the main results presented in this section are still valid.

## 3.2 Continuous Uncertain NN-Queries

The basic observation that the difference of two trajectories can be expressed as a single random variable, along with Theorem 3.1, forms the foundation for constructing the IPAC-NN tree introduced in Section 1, which is what we focus upon now. Without loss of generality, we assume that throughout the duration of the time-interval of interest for a given query **UQ_nn(q)**, $[t_b, t_e]$, each trajectory consists of a single segment (i.e., each object's expected location is along a 2D line segment).

Let $(x_{bi}, y_{bi})$ denote the expected location of the uncertain trajectory $Tr_i^u$ at $t_b$ and, similarly, $(x_{ei}, y_{ei})$ denote the expected location of $Tr_i^u$ at $t_e$. The expected motion of $Tr_i^u$ during $[t_b, t_e]$ will be characterized by a velocity vector whose corresponding $X$ and $Y$ components are:
$v_{xi} = (x_{ei} - x_{bi})/(t_e - t_b)$ and $v_{yi} = (y_{ei} - y_{bi})/(t_e - t_b)$. Hence, the expected location at some time instant $t \in [t_b, t_e]$ will have coordinates:
$x_i(t) = x_{bi} + v_{xi}(t - t_b)$ and $y_i(t) = y_{bi} + v_{yi}(t - t_b)$
which are the coordinates of the center of the uncertainty disk at $t$.

For a given trajectory $Tr_i^u$ which is not the querying tra-

jectory (i.e., $i \neq q$), let $TR_{iq}$ denote the *difference-trajectory* $Tr_i^u - Tr_q^u$. In other words, at each time instant $t$, the expected location of the object moving along $TR_{iq}(t)$ is a vector-difference of the expected locations of the corresponding points along $Tr_i^u(t)$ and $Tr_1^u(t)$. $TR_{iq}(t)$ captures the spirit of Section 3.1, in the sense that the 2D distance between the expected locations of the objects moving along $Tr_i^u(t)$ and $Tr_1^u(t)$ (at time $t$), (cf. [2, 23]) now becomes the distance at that same time $t$ that an object moving along $TR_{iq}$ has from the origin (0,0). Let $V_{xiq} = v_{xi} - v_{xq}$, $V_{yiq} = v_{yi} - v_{yq}$ denote the components of the velocity of the object whose expected trajectory is $TR_{iq}$ and $X_{biq} = x_{bi} - x_{bq}$ and $Y_{biq} = y_{bi} - y_{bq}$ denote the coordinates of the expected location at $t_b$. Then, the distance of $TR_{iq}$ from the origin, as a function of the time is $d_{iq}(t) = \sqrt{At^2 + Bt + C}$, where:
$A = V_x^2{}_{iq} + V_y^2{}_{iq}$,
$B = -2(V_{x_{iq}}^2 t_b + V_{x_{iq}} X_{b_{iq}} + V_{y_{iq}}^2 t_b + V_{y_{iq}} Y_{b_{iq}})$ and
$C = 2X_{b_{iq}} V_{x_{iq}} t_b + V_{x_{iq}}^2 t_b^2 + X_{b_{iq}}^2 + 2Y_{b_{iq}} V_{y_{iq}} t_b + V_{y_{iq}}^2 t_b^2 + Y_{b_{iq}}^2$.
Since $A \geq 0$, the function $d_{iq}(t)$ is a *hyperbola* and, based on the underlying parabola (under the square root), it attains a *minimum* at $t_m = -B/2A$ (if $t_m \notin [t_b, t_e]$, the hyperbola is strictly monotonic).

Given a collection of such distance functions (one for each moving object, except the querying one), based on the observations in Section 3.1, we know that at any time instant $t$, the ranking of the probabilities of a given object $Tr_j^u$ being a nearest neighbor to $Tr_q^u$ is the same as the ranking of the distance functions $d_{iq}(t)$. Hence, the problem of constructing the IPAC-NN tree, which is, determining the member-nodes of each level along with their respective time-intervals, can be reduced to the problem of finding the *collection of (ranked) lower envelopes* for the set of distance functions $\mathcal{S}_{DF} = \{d_{1q}(t), d_{2q}(t), \ldots, d_{Nq}(t)\}$ between $t_b$ and $t_e$. We now focus on describing how to construct the lower envelope of $\mathcal{S}_{DF}$.

Firstly, we observe that two different distance functions, e.g., $d_{iq}(t)$ and $d_{jq}(t)$, in general, can intersect in *at most* two points[2] – consequently, they can have 0, 1 or 2 intersections throughout $[t_b, t_e]$. Their intersections (if any) can be straightforwardly obtained by setting $d_{iq}(t) = d_{jq}(t)$ which, after squaring both sides, amounts to solving a quadratic equation and checking whether each of the solutions (if any) is $\in [t_b, t_e]$. Parts a.) and b.) in Figure 9 illustrate two cases in which pairs of distance functions (corresponding to pairs of $TR$-like trajectories) intersect in 2 and 1 points, respectively. We call such intersection points *critical time-points*. To determine how each of the input-hyperbolae contributes to the lower envelope, it suffices to compare the corresponding distance functions in a single time value $t_{in}$ anywhere in-between two consecutive critical time-points. In the sequel, without loss of generality, we assume an existence of a function called $Env2(TR_{iq}, TR_{jq}, t_1, t_2)$ which takes two difference-trajectories as input and returns their lower envelope as output, along with the critical times, between times $t_1$ and $t_2$. Clearly, $Env2(TR_{iq}, TR_{jq}, t_1, t_2)$ runs in O(1).

**Example 5.** *In the example of Figure 9.a), the outcome of* $Env2(TR_1, TR_2, t_b, t_e)$ *generates the lower envelope* $LE_{1,2} = [(TR_2, [t_b, t_{11}]), (TR_1, [t_{11}, t_{12}]), (TR_2, [t_{12}, t_e])]$. *On the other hand, in the settings of Figure 9.b),* $Env2(TR_3, TR_4, t_b, t_e)$ *yields* $LE_{3,4} = [(TR_4, [t_b, t_{31}]), (TR_3, [t_{31}, t_e])]$.

Now, the main question is how to efficiently construct the lower envelope of the whole collection of distance-trajectories (i.e., the set $\mathcal{S}_{DF}$ of their distance functions to $Tr_q$). The problem of efficiently constructing a lower envelope has already been addressed in the literature [5, 29]. For our settings we implemented a divide-and-conquer based approach, in a spirit of *MergeSort*, that we used in our experiments. The algorithm which constructs the lower envelope for a set of distance-trajectories $\mathcal{S}_{TR} = \{TR_1, TR_2, \ldots, TR_N\}$ (i.e., their distance functions $\mathcal{S}_{DF} = \{d_{1q}(t), d_{2q}(t), \ldots, d_{Nq}(t)\}$) can be specified as follows:

```
Algorithm 1 LE_Alg($\mathcal{S}_{TR}$,1,N)
    Let $C = \lceil N/2 \rceil$
    Merge_LE((LE_Alg($\mathcal{S}_{TR}$,1,C), LE_Alg($\mathcal{S}_{TR}$,C,N))
```

with an additional base case specifying that the output of LE_Alg($\mathcal{S}_{TR}$,i,i) is $[(TR_i, [t_b, t_e])]$.

The main difference with the traditional *MergeSort* algorithm is that, when merging two input-envelopes, instead of incrementing counters and comparing elements of arrays, we *incrementally sweep* over the critical time-points of each of them, and maintain the values of the *current lower bound* and *current upper bound* from among the critical times of the inputs. In addition, when merging two envelopes, denote the operation as $\odot$, we cannot simply *concatenate* them, but we need one more task: namely, if the first (in time) portion of the currently obtained lower envelope is defined by the same $TR_j$ that defines the last portion of the existing envelope, the concatenation will also merge the two consecutive time intervals into one. In other words, the $\odot$-concatenation of $[(TR_j, [t_{j1}, t_{j2}])]$ and $[(TR_j, [t_{j2}, t_{j3}])]$ yields $[(TR_j, [t_{j1}, t_{j3}])]$. For completeness, our implementation of the algorithm for merging two (lower) envelopes is given below:

```
 Algorithm2 Merge_LE($LE_1, LE_2$)
Input: Two lower-envelopes with their critical time-points
$LE_1 =$
$[(TR_{1i_1}, [t_b, t_{11}]), (TR_{1i_2}, [t_{11}, t_{12}]), \ldots, (TR_{1i_m}, [t_{1(m-1)}, t_{1m}])]$
$LE_2 =$
$[(TR_{2i_1}, [t_b, t_{21}]), (TR_{2i_2}, [t_{21}, t_{22}]), \ldots, (TR_{2i_n}, [t_{1(n-1)}, t_{1n}])]$
Output: The combined lower-envelope $LE_{1,2} = LE_1 \uplus LE_2$
Let $LE_{1,2} = \emptyset$;
$k = p = 0$;
while($(k < m) \vee (p < n)$)
{       $t_1^{cl} = t_{1k}$; $t_2^{cl} = t_{2p}$;
        $t_1^{cu} = t_{1(k+1)}$; $t_2^{cu} = t_{2(p+1)}$; // assume $t_{10} = t_{20} = t_b$
        $t^{cl} = max(t_1^{cl}, t_2^{cl})$;       // current lower bound
        $t^{cu} = min(t_1^{cu}, t_2^{cu})$;       // current upper bound
                        // of the sweeping time-interval
        $LE_{1,2} = LE_{1,2} \odot Env2(TR_1 i_k, TR_{2j_r}, t^{cl}, t^{cu})$
            // concatenate ($\odot$) the currently obtained
              // envelope due to the existing one.
        If ($t_1^{cu} < t_2^{cu}$)               k++;
        Else_If ($t_2^{cu} < t_1^{cu}$)        p++;
        Else            // ($t_2^{cu} = t_1^{cu}$)
              { p++; k++; } // advance }
```

Due to the properties of the Davenport-Schinzel sequences (cf. [29]), the combinatorial complexity of the lower envelope is $\lambda_2(N) = 2N - 1 = O(N)$, since two hyperbolae can intersect in at most two points. The time complexity of the Algorithm 2 is linear in the size of the sum of its inputs which, in turn, implies that the time complexity of the Algorithm 1 is specified by the recurrence: $T(2N) = 2T(N) + 2N$. Hence, the complexity of constructing the lower envelope is $O(N \log N)$.

[2] In their intervals of strict monotonicity, they can have at most 1 intersection.

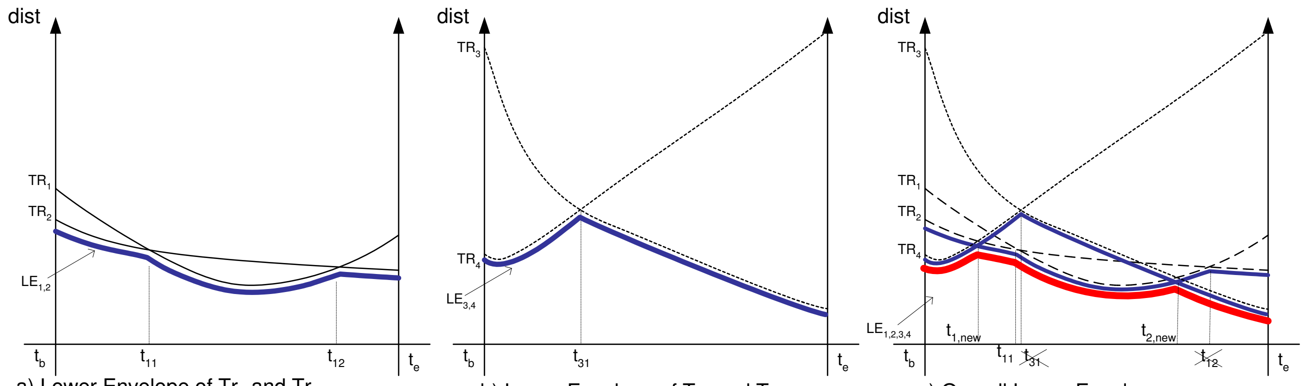

a) Lower Envelope of Tr$_1$ and Tr$_2$ b) Lower Envelope of Tr$_3$ and Tr$_4$ c) Overall Lower Envelope

**Figure 9: Constructing the lower envelope.**

We illustrate the concepts with:

**Example 5.** *Observe Figure 9, and assume that the envelopes in Part a.) and b.) represent the inputs to the Merge_LE. Initially, the current lower bound* $t^{cl}$ *is* $t_b$ *(since* $t_1^{cl} = t_2^{cl} = t_b$*), whereas the current upper bound is* $t^{cu} = min(t_{11}, t_{31}) = t_{11}$. *Hence,* $Env2(TR_2, TR_4, t_b, t_{11})$ *is applied in the first iteration, obtaining a new critical time-point (*$t_{1,new}$*) and generating an envelope with two portions* $(TR_4, [t_b, t_{1,new}])$ *and* $(TR_2, [t_{1,new}, t_{11}])$. *Since* $t_{11} < t_{31}$, *we increment k at the end of the loop which, in turn, means that* $t_1^{cl} = t_{11}$ *and* $t_1^{cu} = t_{12}$. *Consequently, throughout the second iteration of the while-loop we have* $t^{cl} = max(t_1^{cl}(= t_{11}), t_2^{cl}(= t_b)) = t_{11}$ *and* $t^{cu} = min(t_1^{cu}(= t_{12}), t_2^{cu}(= t_{31})) = t_{31}$. $Env2(TR_1, TR_4, t_{11}, t_{31})$, *yields the next part of the overall envelope* $[(TR_1, [t_{11}, t_{31}])]$. *Since* $t_{31} < t_{12}$, *this time we increment p before we enter the next iteration. Subsequent iterations will consecutively invoke:*

*–* $Env2(TR_1, TR_3, t_{31}, t_{12})$, *generating a new critical time-point (*$t_{2,new}$ *in Figure 9.c) and removing* $t_{31}$ *from the list of critical time-points because* $TR_1$ *continues to be the lower envelope at it (cf.* $\odot$*-concatenation). After this iteration,* $LE_{1,2,3,4}$ *consists of* $[(TR_4, [t_b, t_{1,new}])$, $(TR_2, [t_{1,new}, t_{11}])$, $(TR_1, [t_{11}, t_{2,new}])$, $(TR_3, [t_{2,new}, t_{12}])]$*;*

*– Lastly, invoking* $Env2(TR_2, TR_3, t_{12}, t_e)$ *will generate* $[(TR_3, [t_{12}, t_e])]$ *which, when appended to the existing* $LE_{1,2,3,4}$ *"absorbs"* $t_{12}$ *as a critical time point.*

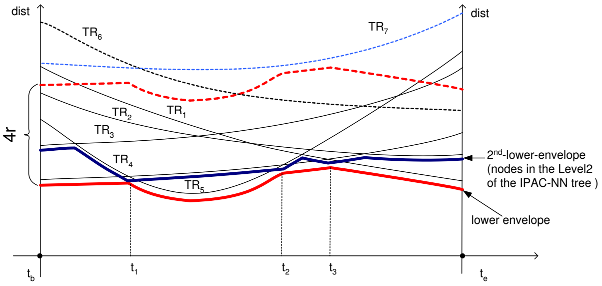

**Figure 10: Envelopes and IPAC-NN tree.**

One of the benefits of constructing the lower envelope is that it provides a *continuous-pruning* criteria. Namely, the trajectories whose distance functions do not intersect the region bounded by the lower envelope and its vertically-translated copy for a vector of length $4r$ in the *(distance,time)* space, can never have a non-zero probability of being a nearest neighbor to $Tr_q^u$. The reason for this is that at any time instant, in order for any (after convolution) object to have a non-zero probability of being a nearest neighbor to (0,0), its nearest location (which is $2r$ closer then the centroid of its convolution) must be no further than $2r$ from the ring centered at the nearest neighbor to (0,0) at that time, and with width $2r$. As an example, in Figure 10, $TR_7$ can be safely pruned from any consideration, because its distance from the lower envelope at any time instant is $> 4r$.

Now, the procedure for constructing the IPAC-NN tree that can be used for answering ranking-based continuous probabilistic NN queries for uncertain trajectories, can be outlined as follows:

```
Algorithm3 Tree_IPAC-NN($\mathcal{T}$, $Tr_q$, $[t_b, t_e]$)
Input: A collection of trajectories $\mathcal{T}$; a querying trajectory
  $Tr_q \in \mathcal{T}$, and a time-interval $[t_b, t_e]$
Output: The IPAC-NN tree for the continuous probabilistic
  NN-query.
1. Construct the lower envelope using Algorithm 2. The
   lower envelope corresponds to the nodes in Level_1 of the
   IPAC-NN tree;
2. Prune all the objects that can never have a non-zero prob-
   ability of being a nearest neighbor;
3. for each level L
4.    for each time-interval bounded by a pair of consecutive
      critical time-points $t_i$ and $t_{i+1}$ on the level $L-1$ envelope
5.       Remove from consideration $TR_i^{L-1}$ defining the
         envelope at level $L-1$ in $(t_i, t_{i+1})$
6.       Construct the portion of the lower-envelope at
         level L applying Algorithm 1.
7.    end_for
8. end_for
```

Since the combinatorial complexity of the lower envelope is $O(N)$, after its construction ($O(N \log N)$), the pruning phase has a time complexity of $O(N^2)$. Assuming that, after the pruning, there are $\lceil N/K \rceil$ objects left for consideration, the running time for constructing the 2nd-lower-envelope (equivalently, the Level_2 nodes of the IPAC-NN tree) is bounded by $O(N\lceil N/K \rceil \log(\lceil N/K \rceil))$. Since two distance function (hyperbolae) can intersect at most twice, we observe that the total number of intersection points within the zone bounded by the lower envelope and it translation for

$4r$ in the *(distance,time)* space is $O(\lceil N/K \rceil^2)$, which is the upper bound on the complexity of (i.e., the number of nodes in) the IPAC-NN tree. Figure 10 illustrates the first two levels of lower envelopes for a given set of (distance functions of) uncertain trajectories.

We summarize the results of this section with the following theorem:

**Theorem 2:** *The graph of all the envelopes in the (distance, time) space that intersect the zone bounded by the lower envelope and its copy vertically translated by $4r$ between times $t_b$ and $t_e$ is the dual of the DAG obtained by removing the root of the IPAC-NN tree corresponding to a given continuous probabilistic NN-query between $t_b$ and $t_e$. The combinatorial complexity of this graph is $O(\lceil N/K \rceil^2)$, which is the combinatorial complexity of the IPAC-NN tree.*

We conclude this section with one last observation regarding the complexity results: the derivations the we presented assumed that all the trajectories have one single segment. However, in case each trajectory has $m$ segments throughout the time-interval of interest for the query, the bounds need to be multiplied by a factor of $Nm$.

## 4. VARIATIONS OF THE NN-QUERY

One of the benefits of our work is that the IPAC-NN tree structure provides a foundation for extending the capabilities of MOD in terms of processing continuous probabilistic NN queries. For example, one can define predicates that will enables the users to pose a query like:

SELECT $T$ FROM MOD
  WHERE EXISTS $Time$ IN $[t1, t2]$
    AND ProbabilityNN$(T, Tr_Q, Time) > 0$

In the rest of this section, we identify four categories of syntactic variants of probabilistic continuous NN-queries that can be answered using an IPAC-NN tree and we outline the algorithms for their processing. Due to space limitations, we do not provide a formal description of the set of predicates expressing the queries, nor corresponding SQL-statements. However, we note that similar formalizations have been presented in [36], albeit for a slightly different purpose (range queries for uncertain trajectories). The claims in this section expressing the complexity results for the queries follow directly from the results in Section 3.

**Category 1:** Queries that pertain to verifying the properties of a single trajectory.

- $UQ_{11}(\exists t)$: *"Does $Tr_i^u$ have a non-zero probability of being a NN to $Tr_q^u$ at some time during $[t_b, t_e]$?"*

In order to answer $UQ_{11}$ it suffices to check whether the (distance function of) $TR_i$ is inside or intersects the boundaries of the zone in-between the lower envelope (Level_1 of the *IPAC-NN* tree) and its $4r$-translated copy.

- $UQ_{12}(\forall t)$: *"Does $Tr_i^u$ have a non-zero probability of being a NN to $Tr_q^u$ all throughout $[t_b, t_e]$?"*

The answer of $UQ_{12}$ can be processed by checking the following conditions: (1) $TR_i$ is inside the pruning-zone at $t_b$; and (2) it stays inside it until $t_e$, i.e., it does *not* intersect the envelope and its $4r$-translated copy, determining the boundaries of the pruning zone.

- $UQ_{13}(X\%$ of $[t_b, t_e])$: *"Does $Tr_i^u$ have a non-zero probability of being a NN to $Tr_q^u$, at least $X\%$ of the time in $[t_b, t_e]$?"*

The main observation for the processing of $UQ_{13}$ is that, in addition to checking for all the intersections, an additional "accumulator" variable is needed to sum up the time-intervals during which $TR_i$ is inside the pruning zone.

**Claim 1:** *The time complexity of processing a Category 1 query is $O(N)$ (i.e., the combinatorial complexity of the lower envelope) after $O(N \log N)$ pre-processing time.*

**Category 2:** These queries extend Category 1 with another parameter, $k$, for the purpose of *ranking* a particular trajectory.

- $UQ_{21}([(\exists t), k])$: *"Does $Tr_i^u$ have a non-zero probability of being a $k^{th}$ highest-probability NN of $Tr_q^u$ at any time in $[t_b, t_e]$?"*

To answer this query, we check whether there exists a node in the *IPAC-NN* tree, at Level_i $i \leq k$, which has $Tr_i^u$ as its label-attribute. Equivalently, we check whether $TR_i$ intersects the Level_i ($i \leq k$) lower envelope.

- $UQ_{22}([(\forall t), k])$: *"Does $Tr_i^u$ have a non-zero probability of being a $k^{th}$ highest-probability NN to $Tr_q^u$ all throughout $[t_b, t_e]$?"*

The answer of $UQ_{22}$ can be processed by: (1) checking whether $TR_i$ is at the Level_i ($i \leq k$) lower envelope at $t_b$; and (2) checking that it maintains that property until $t_e$.

- $UQ_{23}(X\%$ of $[t_b, t_e]$,k): *"Does $Tr_i^u$ have a non-zero probability of being a $k^{th}$ highest-probability NN to $Tr_q^u$, at least $X\%$ of the time in $[t_b, t_e]$?"*

Similarly to $UQ_{13}$, the main observation for the processing of $UQ_{23}$ is that, in addition to checking whether $TR_i$ is initially at the Level_i ($i \leq k$) lower envelope, an "accumulator" variable is used to sum up the time-intervals during which $TR_i$ maintains that property.

Observing that at every Level_j the total combinatorial complexity of the lower envelope is bounded by $O(N)$, we have:

**Claim 2:** *The time complexity of processing a Category 2 query is $O(kN)$ (equal to the combinatorial complexity of the levels of lower envelopes that need to be checked) after $O(\lceil N/K \rceil^2)$ pre-processing time.*

The next two categories of continuous probabilistic NN queries are extensions of Category 1 and Category 2 when we quantify over the space of the uncertain trajectories.

**Category 3:** Queries pertaining to the entire MOD.

- $UQ_{31}(\exists t)$: *"Retrieve all the trajectories that have a non-zero probability of being NN to $Tr_q^u$ some time during $[t_b, t_e]$."*

The answer to this query essentially amounts to constructing the IPAC-NN tree.

- $UQ_{32}(\forall t)$: *"Retrieve all the trajectories that have a non-zero probability of being NN to $Tr_q^u$ throughout the entire $[t_b, t_e]$."*

In addition to constructing the *IPAC-NN* tree (equivalently, the collection of lower envelopes) the processing of $UQ_{33}$ requires checking which $TR_i$ intersects $4r$-translation of the lowest (Level_1) lower envelope – an overhead of $O(N)$.

- $UQ_{33}(X\%$ of $[t_b, t_e])$: *"Retrieve all the trajectories that have a non-zero probability of being NN to $Tr_q^u$ at least $X\%$ of the entire $[t_b, t_e]$."*. In addition to $UQ_{33}$ we now need another "accumulator" variable, that will measure the portion of the time that each trajectory that has intersected the $4r$-translation of the lowest (Level_1) lower envelope, has spent outside of it.

**Claim 3:** *The time complexity of processing a Category 3 query is $O(\lceil N/K \rceil^2)$.*

**Category 4:** The last category of queries that we consider extends Category 3 in the same way as queries from Category 2 extend queries from Category 1 – by adding the value of $k$ as a ranking parameter in terms of $k$-th highest

NN probability. Due to space limitations, we do not formally present these queries here. However, we note that the complexity of their processing introduces an additional factor of $k$ in the $O(\lceil N/K \rceil^2)$ (Claim 3).

We conclude this section with the observation that another variant of $UQ_{11}$ and $UQ_{21}$ and $UQ_{31}$ would consider a *fixed* time value (i.e., $t = t_f$) and evaluate the properties at *that* time, however, the corresponding complexities are the same as the ones expressed the respective claims above.

## 5. EXPERIMENTAL OBSERVATIONS

In this section, we evaluate some benefits of our proposed methodology. Our experiments are implemented in C++ on a Pentium IV 3.60GHZ, 1G MB memory and Windows XP platform. For our experiments, we considered a geographic area of size 40 × 40 miles$^2$. The moving objects were generated using a modified version of the random waypoint model, and each object starts at a randomly selected position in the region of interest. Subsequently, the object picks a random direction and moves at a speed randomly distributed between 15mph and 60mph. For simplicity, we assumed that all the objects change their velocity vectors synchronously. The duration of the motion is fixed to 60min.

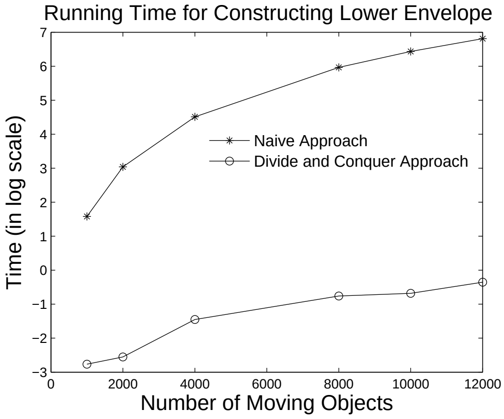

**Figure 11: Construction of Lower Envelope**

In the first group of experiments, we investigate the efficiency of computing the lower envelope of the distance functions, by comparing our approach (cf. Algorithm 1) against the naive approach, which finds the intersection of all the distance functions, sorts them in time, then sweeps in time comparing the lowest values in-between intersections ($O(N^2 \log N)$, since there are $O(N^2)$ such intersections). We varied the number of moving objects from 1000 to 12000 and measured the running time of each approach. The results are plotted in Figure 11, where the running time is shown in a logarithmic scale. As expected based on the theoretical analysis, our approach is much faster, with orders of magnitude speed-up.

Next, we evaluated the efficiency of using our computed lower envelope to answer $UQ_{11}$ and $UQ_{13}$ (cf. Section 5), where we set the value of $X = 50\%$ for $UQ_{13}$. We compared our approach with the naive approach, which checks all pairwise intersection times of the distance functions. Again, the total number of objects was between 1000 and 12000 and we randomly selected an object for the evaluation. The averaged results of 100 such selections are illustrated in Figure 12, which shows that the lower envelope yields significant speedup(s).

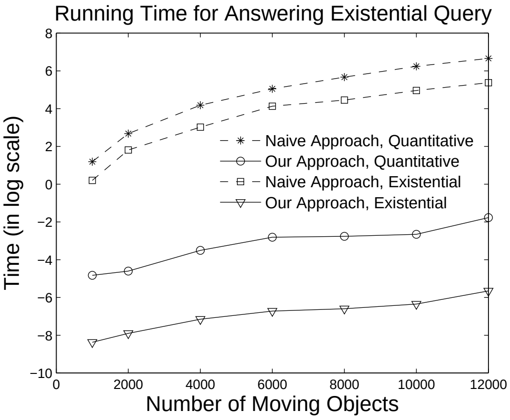

**Figure 12: Existential Queries**

Finally, we evaluated the pruning power of the lower envelope as a function of the uncertainty radius. We varied the radius of uncertainty for the moving objects from 0.1 mile to 2 miles, and measured the ratio when fixing the total number of moving objects to 2,000 and 10,000, respectively. The result is shown in Figure 13. It can be observed that when the moving objects have an uncertainty radius of 0.5 mile, over 90% of the objects can be pruned from any consideration, based on the lower envelope. When the radius increased to mile, about 85% of the objects can be pruned. An implication of this observations is that when actual evaluation of the probabilities is needed, only about 15% of the objects will contribute for an uncertainty radius of 1 mile.

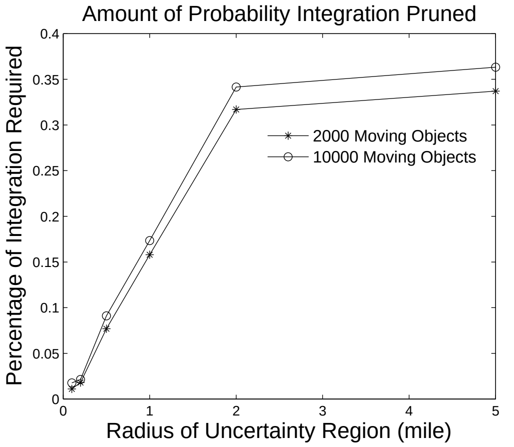

**Figure 13: Pruning Power of the Lower Envelope**

## 6. RELATED WORK

Nearest neighbor queries are essential operations in a wide variety of application domains, from machine learning and computer vision [28] to classification and clustering in data mining [32]. Voronoi diagrams, extensively studied in computational geometry [5, 1], provide a tool for finding the nearest neighbor of a query point among N static points in

$O(\log N)$ query time for 2D. For spatial databases, the problem of efficient scalable processing of (k)NN-queries has been addressed in [24] with a branch-and-bound approach and in [10] with an incremental technique, both relying on R-trees for indexing.

In recent years, there have been many interesting results on (k)NN-queries in spatio-temporal settings. In [15], a dual transformation (points to lines) is explored for developing efficient algorithms when the objects are moving in one dimension. Generic methodologies for processing spatio-temporal queries for trajectories, based on a rich algebra of types, are presented in [16]. The generation of the time-parameterized answer to the continuous variant of the NN-queries, along with the other traditional spatial queries, in spatio-temporal settings, and the efficient scalable processing of such queries based on TPR-trees was presented in [34, 33].

When the motion of the objects is represented as a stream of (location,time) updates, the main issue is how to efficiently monitor and update the answer to (k)NN queries, for which scalable techniques have been proposed in [38, 39]. On the other hand, when the motion of the object is expressed by (location,time,velocity) updates, an incremental approach for processing (k)NN-queries is presented in [13]. In addition, some papers have focused on efficient processing of such queries on road networks [19, 27].

Two works that are very similar in spirit to ours are [2, 23]. Both of them consider the collection of hyperbolae representing the distance functions from a querying object. However, [23] focuses on processing a (k)NN-query but, unlike our approach, does not use the construction of the lower envelope for the purpose of pruning objects that have zero probability of being nearest neighbor to the querying object within a given time interval. The main goal of [2], on the other hand, is scalable processing of regular and reverse NN-queries, focusing on efficient management of modifications (insertions/deletions) and, once again, the uncertainty is not formally addressed.

Various models of uncertainty in spatio-temporal settings, have been considered in the literature. As we mentioned, [22] considers the uncertainty for the *(location,time)* updates model and demonstrates that, under constraint maximal velocity, the spatial zone of the object's whereabouts is an ellipse. The 3D interpretation of that same model ("beads") was presented in [11]. However, the processing of continuous NN-queries under the uncertainty model was not considered. The uncertainty model that we consider in this work has been used for processing range queries in MOD settings [36], where various semantic categories of the (answers to the) queries were presented and geometric concepts were used for their efficient processing. In this paper, we rely on the results in [4] for processing instantaneous NN-queries in uncertain environments and, in a sense, this work provides a continuous extension of it, due to the properties of the convolution for the sum of independent variables.

A recent work addressing a problem similar to the one tackled in this paper is [12], where the goal is to present efficient algorithms for processing continuous kNN-query, for objects moving on road network with uncertain velocity. Inversely to our results, the work in [12] focuses on finding the upper-envelope of the set of distance functions, guaranteeing that a certain object may be one of the $k$ nearest neighbors. However, although there is no formal analysis of the complexity presented, it appears that the construction of the upper envelope takes quadratic time.

## 7. CONCLUSIONS AND FUTURE WORK

We have addressed the problem of continuous NN queries for uncertain trajectories of moving objects, where the uncertainty at any time instant is bounded by a circle with a fixed radius. We have demonstrated that our approach is applicable to a large class of location *pdf*s—those that are rotationally symmetric. For these settings, we have provided a compact structure, the *IPAC-NN* tree, to represent the answer to such queries and we have given algorithmic solution for constructing the geometric dual of this structure. In addition, we have identified several syntactic variants for the continuous probabilistic NN-queries and demonstrated how they can be efficiently answered.

There are several challenges that we plan to address in the future. One of them is to identify the basic properties of the *descriptors* of the probability values in the *IPAC-NN* trees which, in turn, will enable processing of *continuous threshold* NN-queries (e.g., retrieve the objects that have more than 65% probability of being a nearest neighbor within 50% of the time) [3]. Another interesting problem is to design data structures that provide for scalable processing of such uncertain queries, in a spirit similar to the U-trees [35]. In addition, we are planning to address other variants of continuous probabilistic NN queries (e.g., all pairs, reverse) and compare the semantics of traditional *Top-k* NN queries for crisp trajectories with that for uncertain trajectories (cf. [2, 23, 30]). Finally, we plan to allow for different uncertainty zones of the object locations (i.e., circles with different radii), for which a promising foundation is the Voronoi diagram of moving disks [14].

## 8. REFERENCES

[1] F. Aurenhammer. Voronoi diagrams - a survey of a fundamental geometric data structure. *ACM Comput. Surv.*, 23(3), 1991.

[2] R. Benetis, C. Jensen, G. Karciauskas, and S. Saltenis. Nearest and reverse nearest neighbor queries for moving objects. *VLDB J.*, 15(3), 2006.

[3] R. Cheng, J. Chen, M. F. Mokbel, and C.-Y. Chow. Probabilistic verifiers: Evaluating constrained nearest-neighbor queries over uncertain data. In *ICDE*, 2008.

[4] R. Cheng, D. Kalashnikov, and S. Prabhakar. Querying imprecise data in moving objects environments. *IEEE-TKDE*, 16(9), 2003.

[5] M. de Berg, M. van Kreveld, M. Overmars, and O. Schwarzkopf. *Computational geometry: algorithms and applications.* Springer-Verlag, 2001.

[6] Forbes online issue. http://www.forbes.com/home/digitalentertainment /2006/04/13/google-aol-yahoo-cx_rr_0417maps.html.

[7] B. Gnedenko. Course of Probability Theory. Nauka, 1988.

[8] R. Güting and M. Schneider. *Moving Objects Databases.* Morgan Kaufmann, 2005.

[9] M. Hadjieleftheriou, G. Kollios, V. J. Tsotras, and D. Gunopulos. Efficient indexing of spatiotemporal objects. In *EDBT*, 2002.

[10] G. R. Hjaltason and H. Samet. Distance browsing in spatial databases. *ACM TODS*, 24(2), 1999.

[11] K. Hornsby and M. Egenhofer. Modeling moving objects over multiple granularities. *Ann. Math. Artif. Intell.*, 36(1-2), 2002.

[12] Y.-Y. Huand, C.-C. Chen, and C. Lee. Continuous k -nearest neighbor query for moving objects with uncertain velocity. *GeoInformatica*. (to appear).

[13] G. Iwerks, H. Samet, and K. Smith. Maintenance of k-nn and spatial join queries on continuously moving points. *ACM TODS*, 31(2), 2006.

[14] M. Karavelas. Voronoi diagrams for moving disks and applications. In *WADS*, 2001.

[15] G. Kollios, D. Gunopulos, and V. Tsotras. Nearest neighbor queries in a mobile environment. In *STDM*, 1999.

[16] J. Lema, L. Forlizzi, R. Güting, E. Nardeli, and M. Schneider. Algorithms for moving objects databases. *Computing Journal*, 46(6), 2003.

[17] J.S. Lim. *Two-Dimensional Signal and Image Processing* Prentice Hall, 1990.

[18] M. Mokbel, X. Xiong, and W. Aref. Sina: Scalable incremental processing of continuous queries in spatio-temporal databases. In *ACM SIGMOD*, 2004.

[19] K. Mouratidis, M. Yiu, D. Papadias, and N. Mamoulis. Continuous nearest neighbor monitoring in road networks. In *VLDB*, 2006.

[20] P. Olofsson. *Probability, Statistics and Stochastic Processes.* Wiley-Interscience, 2005.

[21] J. Pei, M. Hua, Y. Tao, and X. Lin. Query answering techniques on uncertain and probabilistic data: tutorial summary. In *ACM SIGMOD*, 2008.

[22] D. Pfoser and C. Jensen. Capturing the uncertainty of moving objects representation. In *SSDB*, 1999.

[23] K. Raptopoulou, A. Papadopoulos, and Y. Manolopoulos. Fast nearest-neighbor query processing in moving-object databases. *GeoInformatica*, 7(2), 2003.

[24] N. Roussopoulos, S. Kelley, and F. Vincent. Nearest neighbor queries. In *SIGMOD Conference*, pages 71–79, 1995.

[25] H. Royden. *Real Analysis* Macmillan Co., 1963.

[26] J. Schiller and A. Voisard. *Location-based Services.* Morgan Kaufmann Publishers, 2004.

[27] C. Shahabi, M. Kolahdouzan, and M. Sharifzadeh. A road network embedding technique for k-nearest neighbor search in moving object databases. *GeoInformatica*, 7(3):255–273, 2003.

[28] G. Shakharovich, T. Darrel, and P. I. (eds.). *Nearest-Neighbor Methods in Learning and Vision: Theory and Practice.* MIT Press, 2006.

[29] M. Sharir and P. K. Agarwal. *Davenport-Schinzel Sequences and Their Geometric Applications.* Campbridge University Press, 1995.

[30] M. Soliman, I. Ilyas, and K.-C. Chang. Top-k query processing in uncertain databases. In *ICDE*, 2007.

[31] D. Suciu and N. Dalvi. Foundations of probabilistic answers to queries. In *ACM SIGMOD*, 2005. tutorial.

[32] P.-N. Tan, M. Steinbach, and V. Kumar. *Introduction to Data Mining.* Addison-Wesley, 2005.

[33] Y. Tao and D. Papadias. Spatial queries in dynamic environments. *ACM TODS*, 28(2), 2003.

[34] Y. Tao, D. Papadias, and Q. Shen. Continuous nearest neighbor search. In *VLDB*, 2002.

[35] Y. Tao, X. Xiao, and R. Cheng. Range search on multidimensional uncertain data. *ACM TODS*, 32(3), 2007.

[36] G. Trajcevski, O. Wolfson, K. Hinrichs, and S. Chamberlain. Managing uncertainty in moving objects databases. *ACM TODS*, 29(3), 2004.

[37] O. Wolfson, A. P. Sistla, S. Chamberlain, and Y. Yesha. Updating and querying databases that track mobile units. *Distributed and Parallel Databases*, 7, 1999.

[38] X. Xiong, M. Mokbel, and W. Aref. Sea-cnn: Scalable processing of continuous k-nearest neighbor queries in spatio-temporal databases. In *ICDE*, 2005.

[39] X. Yu, K. Pu, and N. Koudas. Monitoring k-nearest neighbor queries over moving objects. In *ICDE*, 2005.

## 9. APPENDIX

Before we proceed with the outline of the proofs of the claims from Section 2, we briefly note that when a *translation*, e.g., $\overline{s} \mapsto \overline{s}+\overline{w}$ is applied as a transformation to a 2D variable (in the sense of variable substitution), as well as rotation around the center, e.g., $\overline{s} \mapsto \overline{w}(= \rho_{(0,0),\phi}(\overline{w}))$, the Jacobian determinant evaluates to "1".

**Proof:** (of **Property** ) Firstly, observe that $E(\overline{V}_{iq}) = E(\overline{V}_i) + E(-\overline{V}_q)$ simply because $\overline{V}_{iq}$ is the sum of $\overline{V}_i$ and $-\overline{V}_q$. By definition, the centroid of $f$ can be calculated as: $\overline{C}_c = (\int \overline{x}f(\overline{x})d\overline{x})/(\int f(\overline{x})d\overline{x})$. Let us observe separately the:
(1) *Denominator:* by the definition of the convolution, we have: $\int f(\overline{x})d\overline{x}) = \int[[\int g(\overline{u})\cdot h(\overline{x}-\overline{u})d\overline{u})]d\overline{x} =$ ...substitute variables $\overline{x} = \overline{x}+\overline{u}$, noting that $d\overline{x}$ remains the same and the Jacobian is "1" (translation)... $= \int g(\overline{u})d\overline{u} \cdot \int h(\overline{x})d\overline{x} =$ ...since $h$ and $u$ are *pdf*s, each integral evaluates to "1" ... $= 1$.
(2) *Numerator:* Similarly, $\int \overline{x}f(\overline{x})d\overline{x}) = \int \overline{x}[\int g(\overline{u})\cdot h(\overline{x}-\overline{u})d\overline{u})]d\overline{x}$ $=$ ...applying the same substitution: $\overline{x} = \overline{x}+\overline{u}$ ... $= \int(\overline{x}+\overline{u})[\int g(\overline{u}) \cdot h(\overline{x})d\overline{u})]d\overline{x} = ((\int \overline{x}h(\overline{x})d\overline{x}) \int g(\overline{u})d\overline{u}) +$
$((\int \overline{u}g(\overline{u})d\overline{u}) \int h(\overline{x})d\overline{x})$. Observing once again that $\int h(\overline{x})d\overline{x} = \overline{C}_1$ and $\int g(\overline{u})d\overline{u} = \overline{C}_2$, the claim follows. □.

**Proof:** (of **Property 2**) Assume $\overline{P}$ and $\overline{Q}$ are points from the domain of $f$ such that $\|\overline{PC_c} = \overline{QC}_c\|$. Then, there exists a rotation $\rho$ with a center at $\overline{C_c}$ and an angle $\phi$, such that $\rho_{C_c,\phi}(P) = Q$. This can also be viewed as a composition of: (1) translation of $\overline{C}_c$ to the origin; (2) rotation for angle $\phi$; (3) (de)translation back to $\overline{C}_c$).
Observe $f(\overline{P} - \overline{C}_c) =$ ...by Property 1 ... $= f(\overline{P} - (\overline{C}_1 + \overline{C}_2))$. By definition, this is equal to $\int g(\overline{u}) \cdot h(\overline{P} - \overline{C}_1 - \overline{C}_2 - \overline{u})d\overline{u} =$ ...substituting $\overline{u}$ with $\overline{u} - \overline{C}_1$, $d\overline{u}$ remains, and the Jacobijan is "1" ... $= \int g(\overline{u} - \overline{C}_1) \cdot h(\overline{P} - \overline{C}_2 - \overline{u})d\overline{u} =$ ... by the assumed rotational symmetry of $h$, if $Q$ is a point such that $\|\overline{PC}_2 = \overline{QC}_2\|$ ... $= \int g(\overline{u}-\overline{C}_1)\cdot h(\overline{Q}-\overline{C}_2-\overline{u})d\overline{u} =$ ...substituting $\overline{u}$ with $\overline{u}-\overline{C}_1$ ... $= \int g(\overline{u})\cdot h(\overline{Q}-\overline{C}_1-\overline{C}_2-\overline{u})d\overline{u} = f(\overline{Q}-(\overline{C}_1+\overline{C}_2))$. Since the convolution is *translation (shift) invariant* [17], the claim follows.
□

**Proof:** (of **Lemma 1**) It suffices to prove the claim for the *exclusive* NN probabilities (i.e. $P^{NN\_E}_{1,Q} > P^{NN\_E}_{2,Q}$, cf. Section 2.2), because the *joint* NN probability will appear equally in each of $P^{NN}_{1,Q}$ and $P^{NN}_{2,Q}$. Due to the assumption(s), we have that $R^1_{min} < R^2_{min}$ and $R^1_{max} < R^1_{max}$. Appropriately modifying Equation (5), we have:
(I): $P^{NN}_1(Q) = \int_0^\infty pdf^{WD}_1(R_d) \cdot (1 - P^{WD}_2(R_d))dR_d =$
$\int_{R^{min}_1}^{R_{max}1} pdf^{WD}_1(R_d) \cdot (1 - P^{WD}_2(R_d))dR_d$ and, similarly:
(II): $P^{NN}_2(Q) = \int_0^\infty pdf^{WD}_2(R_d) \cdot (1 - P^{WD}_2(R_d))dR_d =$
$\int_{R^{min}_2}^{R^{max}_1} pdf^{WD}_2(R_d) \cdot (1 - P^{WD}_1(R_d))dR_d$.
The claim follows from the observations that for every $\nu$, when evaluating $pdf^{WD}_2(R^{min}_2 + \nu)$ in (II), there exists an equivalent $pdf^{WD}_1(R^{min}_1 + \nu)$ which, however, is multiplied by a larger value of $(1 - P^{WD}_2(R_d)$ in (I). □